Transfer-matrix simulations of field emission from bundles of open and closed (5,5) carbon nanotubes

A. Mayer, [1,*] N. M. Miskovsky,[2] P. H. Cutler,[2] and Ph. Lambin[1]
[1]*Laboratoire de Physique du Solide, Facultés Universitaires Notre-Dame de la Paix, Rue de Bruxelles 61, B-5000 Namur, Belgium*
[2]*Department of Physics, 104 Davey Lab, Penn State University, University Park, Pennsylvania 16802, USA*
(Received 22 April 2003; revised manuscript received 11 July 2003; published 2 December 2003)

We present simulations of field emission from bundles of metallic (5,5) carbon nanotubes, which are either ideally open or closed. The scattering calculations are achieved using a transfer-matrix methodology for consideration of three-dimensional aspects of both the emitting structure and the surface barrier. Band-structure effects are reproduced by using pseudopotentials and enforcing the incident states to first travel through a periodic repetition of the tubes' basic cell before entering the region containing the fields. The bundles consist of three and six identical structures, which are placed at the corners of equilateral triangles. In all cases, the closed emitters are found to emit less current than the open ones and to be more sensitive to the electric field in their response to neighboring tubes. Due to the enhanced screening of the electric field, the bundles' emission rates are reduced compared to those of the isolated tubes. It turns out that the rates characterizing bundle and isolated emitters are related by a simple formula, whose dependence on the electric field suggests deviations from the Fowler-Nordheim equation at high fields. Finally, the position of peaks associated with quasilocalized states on top of the closed emitters appears to be a strong indicator of the tubes' environment.

DOI: 10.1103/PhysRevB.68.235401 PACS number(s): 73.63.Fg, 79.70.+q, 85.35.Kt, 03.65.Nk

I. INTRODUCTION

Carbon nanotubes show interesting field-emission properties such as low extraction field (macroscopic values of the order of a few volts per micron) and high current densities. In general, their current-voltage characteristics are found to follow a Fowler-Nordheim-type tunneling law[1–4] with an emitter work function around 5 eV depending on the type of nanotube. Electronic states localized near or at the apex of the nanotube influence the current emission profile.[5,6] These localized states are relatively well documented for various kinds of tube termination[7–10] and can be induced by the extraction field.[11] It is assumed in most calculations that the dangling bonds are not saturated, although it is recognized that in ambient conditions hydrogen may saturate them.[12]

In field emission devices, carbon nanotubes are not isolated but entangled with many others or grown in arrays. Their emission properties are modified because of the strong dependence of the local extraction field on the tubes' environment.[13,14] It was established by Nilsson *et al.*[13] that the optimal spacing between aligned nanotubes is approximately twice their length. In an extension of previous publications,[15–21] we consider here the conditions of close proximity that characterize bundles of nanotubes. It was already shown by Lovall *et al.*[22] that the bundles' emission is dominated by the protruding tube. We will consider the complementary situation where the nanotubes have all the same length and compare the emission properties of these ideal bundles with those of their isolated components.

To achieve this objective, we solve the Schrödinger equation[23,24] with a three-dimensional potential representative of both the emitters' structure and the surface barrier. The potential energy is calculated using the techniques of Ref. 25 with improvements described in this paper as well as the Bachelet *et al.*[26] pseudopotential for the representation of carbon atoms. Band-structure effects are included in the energy distributions by enforcing the incident states to first travel through the periodic repetition of the emitters' basic cell before entering the region containing the fields.

The main features of our model are described in Sec. II. Section III then presents results of field emission from metallic (5,5) nanotubes, which are either isolated or in bundles, ideally open or closed. The bundles are described by three or six identical structures placed with a spacing of 0.32 nm at the corners of equilateral triangles. In all cases, the closed emitters are found to emit less current than the open ones and to be more sensitive to the electric field in their response to neighboring tubes. Due to the enhanced screening of the electric field, the bundles' emission rates are reduced compared to those of the isolated tubes. As established in Sec. IV, these rates are related by a simple formula, whose dependence on the electric field suggests deviations from the Fowler-Nordheim equation at high fields. Finally, the position of peaks associated with quasilocalized states on top of the closed (5,5) nanotubes turns out to be a strong indicator of the tubes' environment.

II. THEORY

The geometry considered in this paper is depicted in Fig. 1. The nanotubes are located between a metallic substrate (region I, $z \leqslant -N \times a$) and the field-free vacuum (region III, $z \geqslant D$). The intermediate region consists of a field-free region ($-a \times N \leqslant z \leqslant 0$), which contains N periodic repetitions of the nanotubes' basic cell, and region II ($0 \leqslant z \leqslant D$), which contains the part of the nanotubes subject to the extraction field F. The purpose of the $-a \times N \leqslant z \leqslant 0$ region is to reproduce appropriate band-structure effects in the distribution of incident states. This part of the model is not related to an experimental picture, where nonzero fields would remain up to the metallic substrate. For each simulation, we consider a

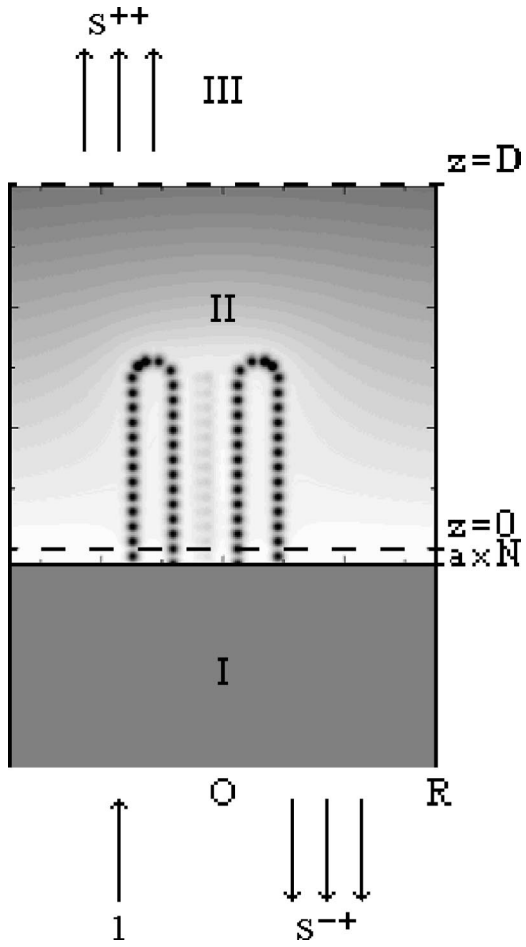

FIG. 1. Schematic depicting of the model. Region I ($z \leqslant -aN$) is a perfect metal. The intermediate region $-aN \leqslant z \leqslant 0$ contains N periodic repetitions of the nanotubes' basic cell (only one cell is represented). Region II ($0 \leqslant z \leqslant D$) contains the part of the nanotubes subject to the extraction field. Region III ($z \geqslant D$) is the field-free vacuum. The arrows in regions I and III symbolize scattering solutions, with a single incident state in region I and the corresponding reflected and transmitted states (whose coefficients are contained in the transfer matrices $\mathbf{S}^{-+}$ and $\mathbf{S}^{++}$, respectively).

distance $D=V/F$, where V is the electric bias between regions I and III (we consider a fixed value of 12 V).

The potential energy in region II is calculated by using techniques described in previous publications.[15] For each carbon atom, we use the Bachelet *et al.* pseudopotential[26] to represent the ion-core potential while Gaussian distributions are used for the remaining electronic densities. These two contributions are displaced rigidly from both sides of the atomic position, according to the polarization $\mathbf{p}_j$ of the atom for which they are representative. The atomic polarizations $\{\mathbf{p}_j\}$ are calculated[23] by taking account of the extraction field, direct dipole-dipole interactions, as well as indirect interactions with images. These image interactions indeed insure the cancellation of the electric field in the region $z \leqslant 0$. In order for the model to be consistent, the $z=0$ plane has to describe a mirror symmetry of the basic cell used to construct the nanotubes [in the case of (n,n) structures, this plane has to contain (unpolarized) atoms]. We neglect any influence that the anode may have on the nanotube (through additional image contributions to the potential energy), as these effects are negligible in experimental conditions. Following Ref. 27, we use a polarizability tensor $\boldsymbol{\alpha}_j/(4\pi\epsilon_0)$ whose main components are 3.0, 0.865, and 0.865 Å^3. Finally, the exchange contribution to the potential energy is calculated within the local-density approximation.[25]

The electronic scattering from the metallic substrate to the vacuum is calculated by the transfer-matrix technique described in Refs. 23 and 24. In this formulation, the electrons are confined inside a cylinder of radius R (chosen large enough so that the results are independent of its particular value). Making use of the cylindrical symmetry of the problem, the wave function is expanded in terms of basis states $\Psi^{\mathrm{I},\pm}_{m,j}=A_{m,j}J_m(k_{m,j}\rho)\exp(im\phi)\exp[\pm i\sqrt{(2m/\hbar^2)E-V_{\mathrm{met}}}z]$ in region I and $\Psi^{\mathrm{III},\pm}_{m,j}=A_{m,j}J_m(k_{m,j}\rho)\exp(im\phi)\times\exp[\pm i\sqrt{(2m/\hbar^2)E}z]$ in region III. In these expressions, the $A_{m,j}$ are normalization coefficients, J_m are Bessel functions, $k_{m,j}$ are transverse wave-vector solutions of $J_m(k_{m,j}R)=0$, E is the electron energy, and V_{met} is the potential energy in the supporting metal. The $\pm$ signs refer to the propagation direction relative to the z axis, which is oriented from region I to region III. The transfer-matrix methodology[23] then provides scattering solutions of the form

$$\Psi^{+}_{m,j} \overset{z\leqslant -a\times N}{=} \Psi^{\mathrm{I},+}_{m,j}+\sum_{m',j'} S^{-+}_{(m',j'),(m,j)}\Psi^{\mathrm{I},-}_{m',j'}$$

$$\overset{z\geqslant D}{=} \sum_{m',j'} S^{++}_{(m',j'),(m,j)}\Psi^{\mathrm{III},+}_{m',j'}, \qquad (1)$$

corresponding to single incident states $\Psi^{\mathrm{I},+}_{m,j}$ in the metallic substrate (the $\mathbf{S}^{-+}$ and $\mathbf{S}^{++}$ matrices are defined in Fig. 1). Total current densities result from the contribution of every solution associated with a propagative incident state in the supporting metal. The procedure is not self-consistent, as we do not consider the corrections that these scattering solutions should induce on the potential energy.

III. APPLICATION: FIELD EMISSION FROM BUNDLES OF OPEN AND CLOSED (5,5) CARBON NANOTUBES

We investigated in previous publications[16–20] the transport and field-emission properties of metallic (5,5) carbon nanotubes. Our model reproduces the constant density of states around the Fermi level as well as peaks associated with van Hove singularities in the distribution of incident states.[17] For the small tube lengths considered, we could observe oscillations in the energy distribution of both incident and field-emitted states, which come from stationary waves in the structure.[16,17,28] Closing the nanotube introduces a quasilocalized state on top of the emitter, which has observable effects in the energy distribution of emitted electrons.[16] It also increases the screening of the electric field and reduces the emission. Saturating the dangling bonds of open tubes with hydrogen reduces the width and height of the potential barrier, which tends to increase the emission.[16] Using a pho-

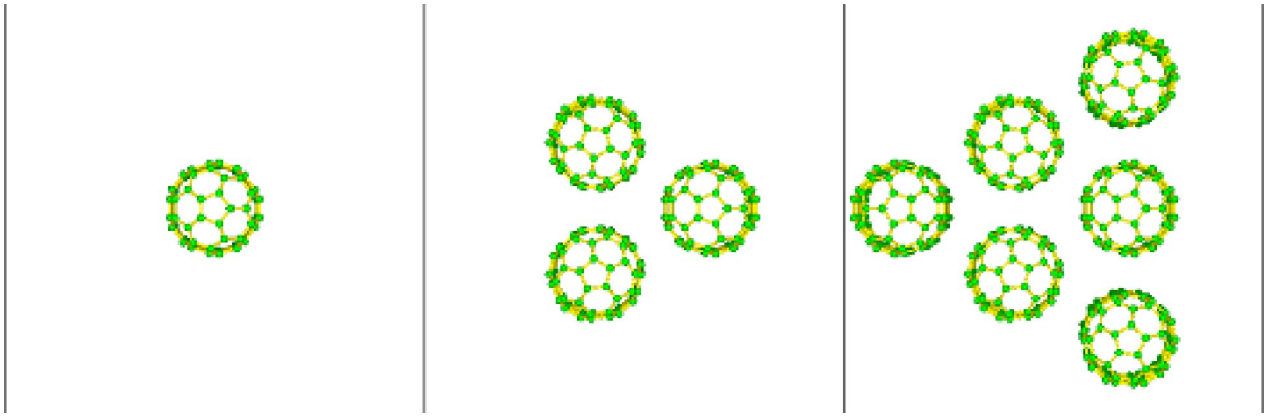

FIG. 2. Representation of bundles of one, three, and six closed (5,5) carbon nanotubes.

tonic stimulation, a further amplification of the current is achieved.[19]

In this paper, we investigate how the emission properties of ideally open and closed (5,5) carbon nanotubes are affected by the close proximity of identical structures, in the conditions characterizing bundles of nanotubes. The bundles we consider consist of three or six identical (5,5) structures placed with a spacing of 0.32 nm at the corners of equilateral triangles (see Fig. 2). Each nanotube consists of $N=16$ basics cells (320 atoms) in the region $-Na \leqslant z \leqslant 0$ and 11 cells (220 atoms) in the region $0 \leqslant z \leqslant D$. The length of these two parts of the nanotube is 3.935 nm and 2.705 nm, respectively (the radius is 0.339 nm). Thirty additional atoms are used to close the structure. For the metallic substrate $z \leqslant -Na$ to reflect the properties of infinite nanotubes, it is given an internal potential energy and a Fermi level of -16 and -5.25 eV, respectively (compared to the vacuum level). The simulations assume *local* extraction fields of 1, 1.5, and 2 V/nm. These values have to be considered as already magnified by a micron-long body in order to account for the difference with macroscopic values (of the order of a few volts per micron). Finally, a temperature T of 298 K is assumed.

A. Field emission from isolated open and closed (5,5) nanotubes

The potential energy associated with isolated open and closed (5,5) nanotubes is illustrated in Fig. 3. The representation corresponds to an applied electric field of 2 V/nm and the equipotentials are labeled by integer values in eV. The total-energy distribution characterizing the electrons emitted from these two structures, for applied electric fields of 1, 1.5, and 2 V/nm, are represented in Fig. 4. The difference with previously published results[20] comes from the longer tube lengths, the lower fields, and the atoms being translated so that the $z=0$ plane here corresponds to a reflection symmetry of the tubes' basic cell.

The energy distributions characterizing the two emitters are similar, except for the sharp peak at -1.45 eV for the 2 V/nm field, which is associated with a quasilocalized state on top of the closed emitter (similar peaks are frequently encountered with capped structures[7,8,11]). As will appear later, the position of this peak is highly sensitive to the tubes' environment, while the other features of the energy distributions present fewer variations when bundles are considered. Considering shorter tubes makes this peak move to higher energies, since one then reduces the field penetration in the

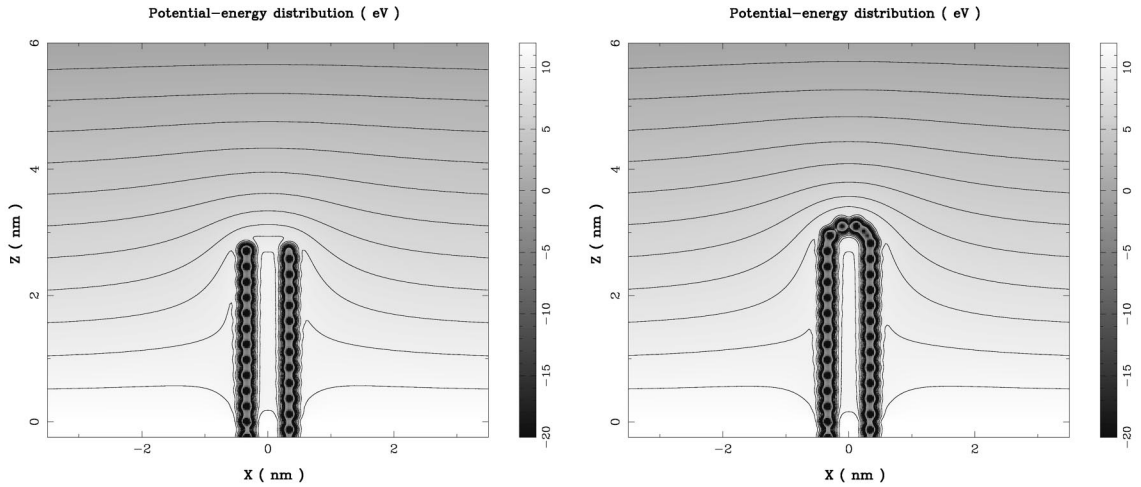

FIG. 3. Potential-energy distribution (section in the xz plane) associated with single open (left) and closed (right) (5,5) nanotubes, for an applied electric field of 2 V/nm. The tubes' basic cell that appears below $z=0$ is repeated 16 times.

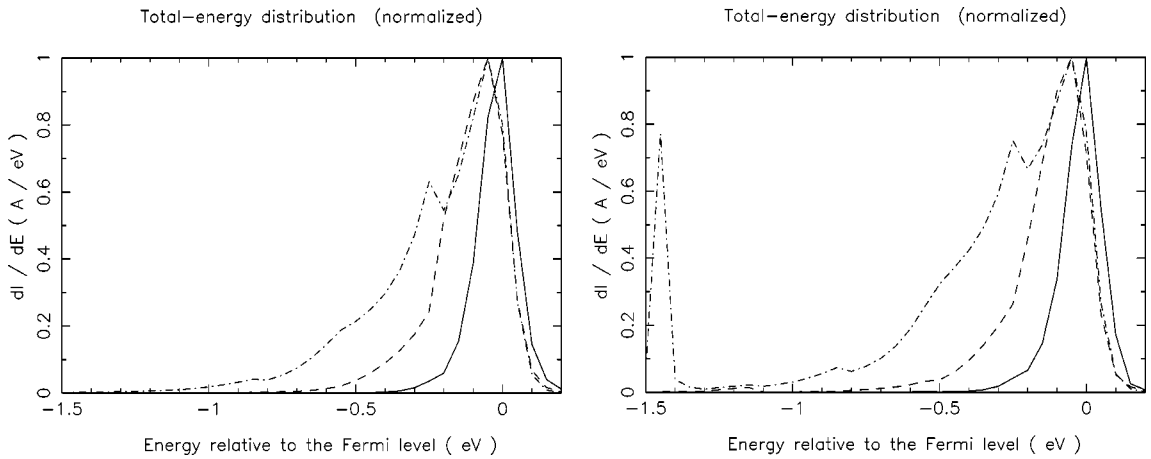

FIG. 4. Total-energy distribution (normalized) of electrons field-emitted from single open (left) and closed (right) (5,5) nanotubes. The extraction field associated with the three curves is 1 (solid), 1.5 (dashed), and 2 (dot-dashed) V/nm. The maximal intensities are 0.617×10^{-19}, 0.221×10^{-10}, and 0.345×10^{-7} A/eV (left) and 0.302×10^{-20}, 0.729×10^{-12}, and 0.911×10^{-9} A/eV (right).

structure (which is responsible for the peaks' displacement towards lower energies). In all cases, there is a significant contribution around the Fermi level and the two structures exhibit the same peaks around -0.85, -0.55, and -0.25 eV (for the 2 V/nm field). These peaks are related to stationary states in the cylindrical part of the open and closed nanotubes. They are closer than observed previously[20] because of the larger tube lengths, and less pronounced because of the electric fields being lower and filtering therefore the energy distributions more strongly.

The currents extracted for the three values of the electric field are 9.69×10^{-21}, 5.51×10^{-12}, and 1.24×10^{-8} A for the open emitter and 4.65×10^{-22}, 1.82×10^{-13}, and 4.36×10^{-10} A for the closed one. These values as well as those calculated hereafter are reproduced in Table I. On average, closing the (5,5) nanotube hence reduces its emission by a factor of 26. This reduced emission was predicted by other authors.[5,11,29] It is the result of several factors, including the potential barrier, the reduced emission area of the closed (5,5) nanotube, and the cap's influence on the direction and supply function of the incident states when encountering the surface barrier.

To enable a more quantitative discussion of the potential energy relevant to the open and closed nanotubes, we represented in Fig. 5 the values computed on the tubes' central axis ($x=y=0$) as well as along their cylindrical body ($x=0.339$ nm, $y=0$). These potential-energy values are calculated using the model of Sec. II for describing the action of the nanotubes' nuclei and valence electrons on the emitted electron when present on that particular axis (the emission current of course depends on the whole three-dimensional distribution). The representation does not include self-consistent corrections associated with the emitted electron (i.e., contributions due to the π electron densities). Unlike the second representation, that associated with $x=y=0$ does not go through any atom of the two structures. The carbon atoms indeed lie on the nanotubes' cylindrical body or hemispherical cap, and the dip that appears at $z=3.098$ nm is due to the ion-core potential of atoms situated on the last pentagonal ring of the closed nanotube (the $x=y=0$ axis goes through its middle). In this first representation, the separation between the internal and external regions of the nanotubes is at $z=2.705$ and 3.098 nm, respectively. We see that the potential is essentially constant inside the nanotube (reflecting the screening of the external field) and that it decreases outside. The transition in the potential at $z=0$ is related to the fact that a finite distance is required (on both sides of the nanotube) to cancel the external field on its central axis. The width of that transition is proportional to the tube's radius. In the second representation, the atomic potentials are more pronounced as carbon atoms are encountered here. The additional potential well that appears with the closed nanotube comes from atoms in the cap. The horizontal alignment of the ion-core potentials reflects the screening of the external field. Outside the nanotubes and beyond the range of the ion-core potentials (i.e., for $z>3.25$ nm), we see that the

TABLE I. Total current (in amperes) extracted from bundles of one, three, or six (5,5) nanotubes, for either open or closed configurations and extraction fields of 1, 1.5, and 2 V/nm.

	One tube		Bundle of three		Bundle of six	
	open	closed	open	closed	open	closed
1 V/nm	9.69×10^{-21}	4.65×10^{-22}	7.55×10^{-22}	2.24×10^{-23}	1.36×10^{-22}	4.34×10^{-24}
1.5 V/nm	5.51×10^{-12}	1.82×10^{-13}	3.82×10^{-13}	1.56×10^{-14}	7.81×10^{-14}	3.68×10^{-15}
2 V/nm	1.24×10^{-8}	4.36×10^{-10}	1.58×10^{-9}	8.01×10^{-11}	4.48×10^{-10}	2.99×10^{-11}

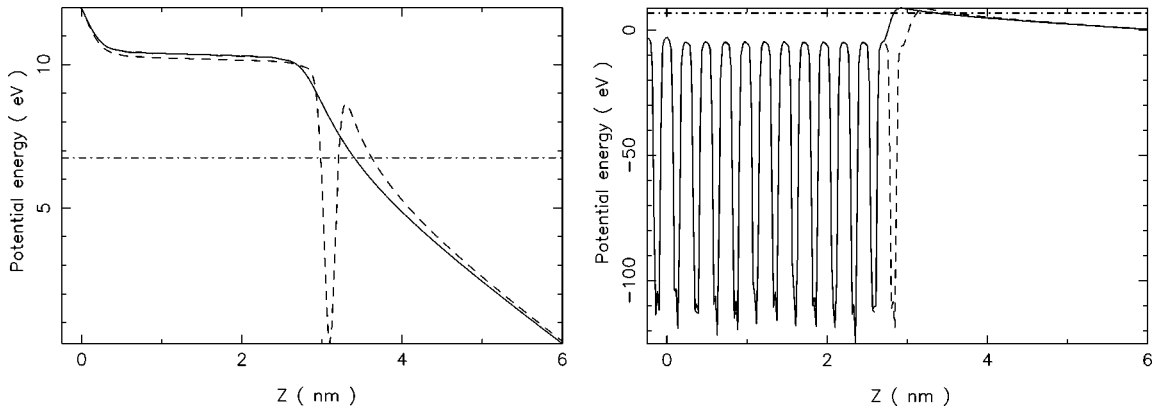

FIG. 5. Potential energy along the $x=y=0$ (left) and $x=0.339$ nm, $y=0$ (right) lines of isolated open (solid) and closed (dashed) (5,5) nanotubes, for an applied electric field of 2 V/nm. Atoms are only met in the right part. The limit between the internal and external parts of the nanotubes in the left part is encountered at $z=2.705$ and 3.098 nm, respectively. The dot-dashed line stands for the Fermi level.

potential energy is higher for the closed nanotube than for the open one. This is a consequence of the higher length and screening capacity of the closed structure, which strains the equipotentials to surround the emitter more strongly than if it were open. As appears in Fig. 3, the equipotentials are more compressed on top of the closed structure (reflecting the enhancement of the field), so that the distance over which the electrons have to tunnel before being emitted is smaller than for the open tube. As the emission from the closed nanotube is, however, reduced compared to the open one (while we expect a higher emission probability from the last atoms if the propagation direction is towards the minimal barrier width), our results suggest that a significant effect of the cap is to reduce the supply function of electrons encountering the apex (through internal reflections) or to lead the electronic flow to a direction unfavorable for emission.

The field-enhancement factors γ, as derived from the slope of the Fowler-Nordheim[30,31] representation of our data, are 1.54 for the open tube and 1.56 for the closed one. These values are obtained by representing $\ln[J/F^2]$ as a function of $1/F$, where $J=I/S$ is the current density associated with the applied electric field F. Expressing J in A/m^2, F in V/m, and the work function ϕ in eV, the coefficient b of the linear fit $\ln[J/F^2]=a-b/F$ of our data is given by $b=6.83\times10^9\phi^{3/2}/\gamma$, which enables one to derive the field-enhancement factor γ (ϕ is 5.25 eV and $S=\pi R^2$ only affects a). As explained in Refs. 20, 32, and 33, the numbers found using that procedure are only indicators of the dependence of the current on the applied electric field and should not be interpreted literally. The actual field-enhancement factor, as derived from a direct calculation of the electric field, is a quantity that depends strongly on the position. Choosing as a reference the point situated on the tubes' axis at a distance of 0.25 nm from the apex, we find a field-enhancement factor of 2.60 for the open tube and 3.80 for the closed one. These values as well as those calculated hereafter are reproduced in Table II.

B. Field emission from bundles of three open and closed (5,5) nanotubes

We now consider three identical (5,5) nanotubes, which are either open or closed and placed with a spacing of 0.32 nm at the corners of an equilateral triangle (see Fig. 2). We represented in Fig. 6 a section of the potential energy, which crosses one of the nanotubes and avoids the two others. As expected, this close proximity between the emitters enhances the screening of the electric field. This is reflected by the fact that the facing equipotential is at 9 eV instead of 8 eV in the previous case.

The total-energy distribution of the field-emitted electrons is represented in Fig. 7. Because of the reduced field penetration, the surface barrier is higher and wider. As a consequence, the energy distributions are thinner and the peaks associated with stationary states still less pronounced. They are, however, at the same position, which is consistent with the fact that they are associated with the body of the tubes where the electric field is canceled. The sharp peak associated with the quasilocalized state on top of the closed structures is displaced here to higher energies by 0.45 eV. This large displacement towards positive values is due to the reduction of field penetration, which causes the emitter apex to be at a higher potential (as reflected by the facing equipotential being at 9 eV instead of 8). It appears, therefore, that the position of peaks associated with quasilocalized states on top of closed emitters is a strong indicator of their environment (through the neighborhood's effect on the local field).

The currents extracted for the three values of the electric field are 7.55×10^{-22}, 3.82×10^{-13}, and 1.58×10^{-9} A for the open emitters and 2.24×10^{-23}, 1.56×10^{-14}, and 8.01×10^{-11} A for the closed ones. Despite the fact that in all cases there are three emitters instead of one, on average the

TABLE II. Field-enhancement factor, as obtained from a direct calculation of the electric field 0.25 nm above the emitter and as derived from the Fowler-Nordheim analysis of our *I-V* data (in parentheses). Note that the Fowler-Nordheim analysis provides a single value for a given structure.

	One tube	Bundle of three	Bundle of six	
			innertubes	outer tubes
open	2.60 (1.53)	2.38 (1.52)	2.13 (1.49)	2.28 (1.49)
closed	3.80 (1.55)	3.54 (1.49)	2.10 (1.45)	3.54 (1.45)

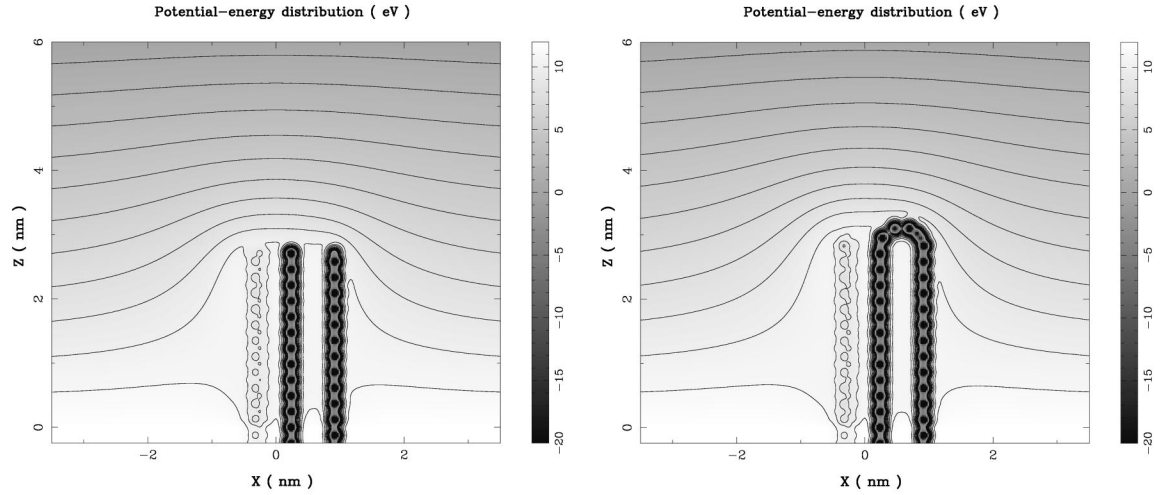

FIG. 6. Potential-energy distribution (section in the *xz* plane) associated with bundles of three open (left) and closed (right) (5,5) nanotubes, for an applied electric field of 2 V/nm. The tubes' basic cell that appears below $z=0$ is repeated 16 times.

total emission is reduced by a factor of 12 (see Table I). This means that each nanotube in the bundle emits 36 times less current than if it were isolated. The emission from a given (5,5) open tube is therefore more affected by the close proximity of other tubes than by the half C_{60} used to close it (reduction of its emission by a factor of 36 rather than 26). However, three open nanotubes, taken together, emit more current than a single closed tube (but less than a single open one). It can be noted that the dispersion around this average value of 12 is larger for the closed nanotubes than for the open ones. Indeed, the reduction factors associated with the three values of the extraction field are 20.8, 11.7, and 5.44, respectively, for the closed structures, while they are 13.2, 14.4, and 7.85 for the open ones. This dispersion is better illustrated in Fig. 10. The fact that the dispersion is higher for the closed nanotubes is due to the fact that the electric field has a stronger influence on the apex of closed structures than on the upper border of the open ones (because of the apex's advanced position in the barrier). When increasing the electric field, the potential barrier at the apex therefore tends faster to the barrier characterizing isolated structures (resulting in stronger variations in the reduction factors).

From the Fowler-Nordheim representation of our data and using the procedure described previously, one can derive field-enhancement factors γ of 1.52 and 1.49 for the open and closed structures, respectively. The values found from a direct calculation of the electric field 0.25 nm above the emitters are 2.38 for the open tubes and 3.54 for the closed ones. The field-enhancement factors obtained from a direct calculation of the electric field are hence more representative of the tubes' environment than the values derived from the Fowler-Nordheim analysis of our data (see Table II for a comparison with previous values).

C. Field emission from bundles of six open and closed (5,5) nanotubes

We finally consider bundles of six open or closed (5,5) nanotubes. As depicted in Fig. 2, they are placed at the cor-

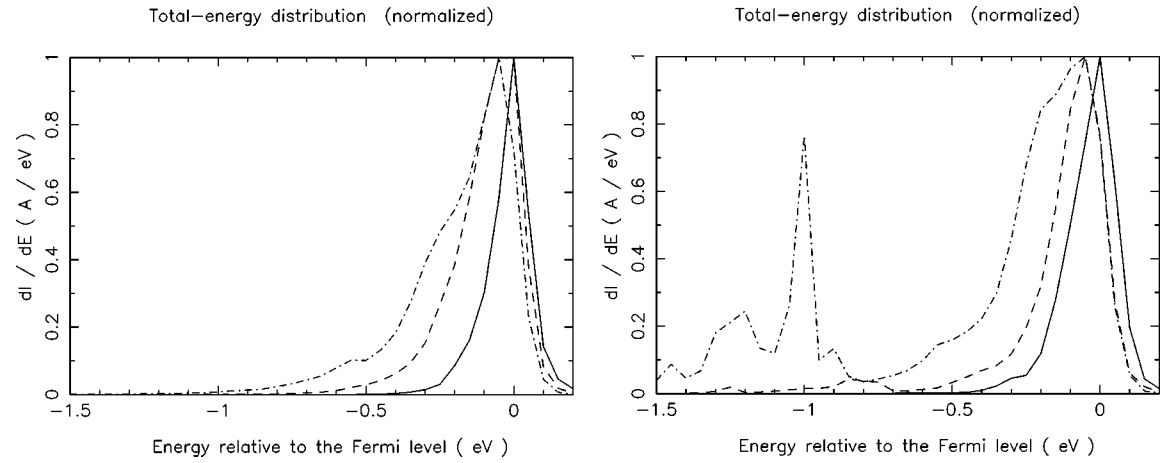

FIG. 7. Total-energy distribution (normalized) of electrons field-emitted from bundles of three open (left) and closed (right) (5,5) nanotubes. The extraction field associated with the three curves is 1 (solid), 1.5 (dashed), and 2 (dot-dashed) V/nm. The maximal intensities are 0.528×10^{-20}, 0.155×10^{-11}, and 0.527×10^{-8} A/eV (left) and 0.123×10^{-21}, 0.670×10^{-13}, and 0.170×10^{-9} A/eV (right).

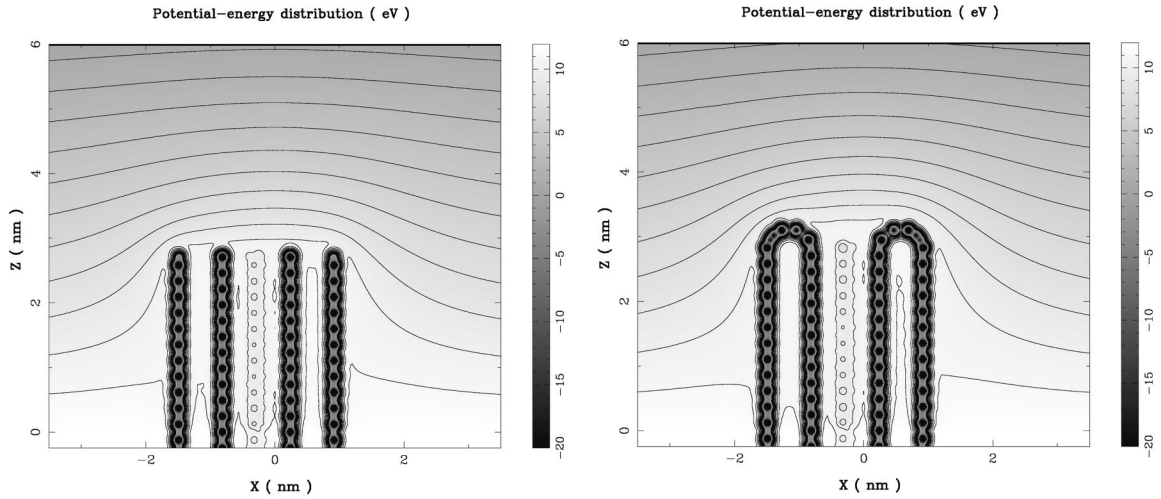

FIG. 8. Potential-energy distribution (section in the *xz* plane) associated with bundles of six open (left) and closed (right) (5,5) nanotubes, for an applied electric field of 2 V/nm. The tubes' basic cell that appears below $z=0$ is repeated 16 times.

ners of equilateral triangles with the same spacing of 0.32 nm. The threefold symmetry characterizing this particular configuration is consistent with the observations of Lovall *et al.*, whose current distributions exhibit this same symmetry.[22] The *xz* plane chosen for the representation of the potential energy in Fig. 8 crosses two nanotubes and avoids the four others. By inspection of this figure, it turns out that the screening of the electric field is still more pronounced than for the two previous configurations since the facing equipotential is at 10 eV instead of 8 and 9 previously.

The total-energy distributions obtained for applied electric fields of 1, 1.5, and 2 V/nm are represented in Fig. 9. The distributions are thinner and the features associated with stationary waves still less pronounced than previously. This is a consequence of the higher surface barrier, which operates a stronger filtering of the escaping states. The most visible change is the position of the peaks associated with the quasilocalized state, whose main contribution moves from -1 to -0.8 eV for the 2 V/nm field value. This displacement towards positive values is again related to the electrostatic interactions between the tubes, which enhance the screening of the electric field and therefore raise the potential at their apex. Because the peaks are now sufficiently close to the Fermi level where significant emission occurs, they also appear at lower field values and the relation between the peaks' position and the field appears more clearly (i.e., displacement to lower energies as the field increases).

The total currents extracted for the three values of the electric field are 1.36×10^{-22}, 7.81×10^{-14}, and 4.48×10^{-10} A for the open structures and 4.34×10^{-24}, 3.68×10^{-15}, and 2.99×10^{-11} A for the closed ones. The total emission is reduced by a mean factor of 3.9 compared to the situation where only three identical structures were considered (see Table I). On average, a given nanotube in a bundle of six therefore emits around eight times less current than the

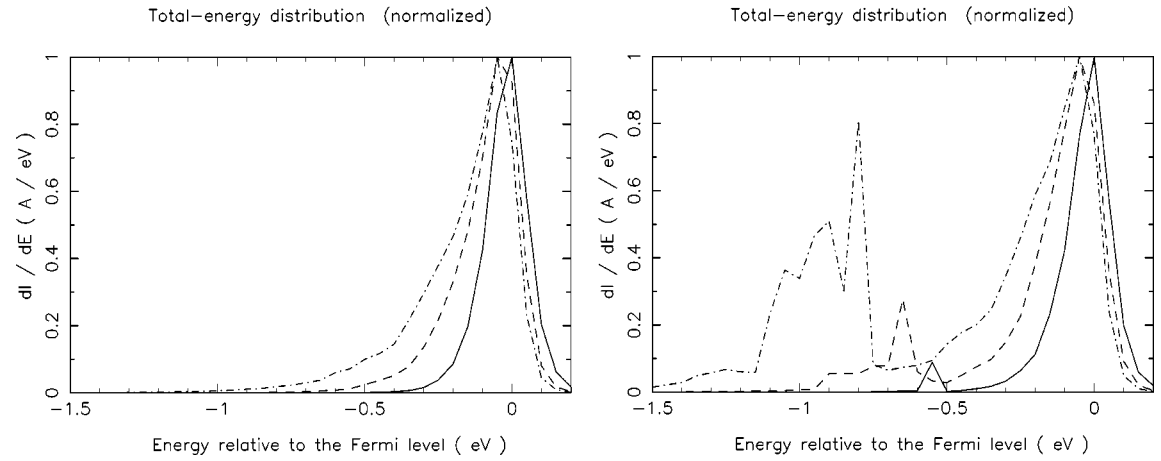

FIG. 9. Total-energy distribution (normalized) of electrons field-emitted from bundles of six open (left) and closed (right) (5,5) nanotubes. The extraction field associated with the three curves is 1 (solid), 1.5 (dashed), and 2 (dot-dashed) V/nm. The maximal intensities are 0.786×10^{-21}, 0.351×10^{-12}, and 0.166×10^{-8} A/eV (left) and 0.240×10^{-22}, 0.135×10^{-13}, and 0.644×10^{-10} A/eV (right).

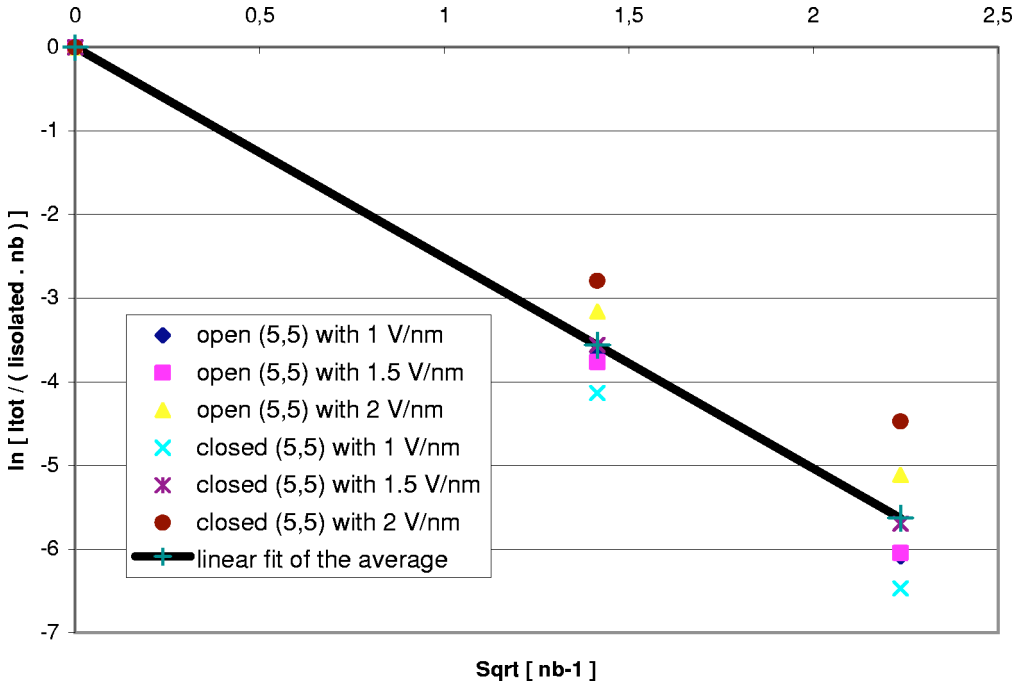

FIG. 10. Representation of $\ln[I_{\text{tot}}/(I_{\text{isolated}}nb)]$ as a function of $\sqrt{nb-1}$, where nb is the number of tubes in each bundle, I_{tot} its total emission, and I_{isolated} the emission obtained with a single tube. The data correspond to open and closed (5,5) nanotubes subject to extraction fields of 1, 1.5, and 2 V/nm. The solid line stands for the best linear fit of these data.

same tube in a bundle of three, and around $6\times3.9\times12 \simeq 280$ times less current than an isolated tube.

The Fowler-Nordheim analysis of these data provides field-enhancement factors γ of 1.49 and 1.45 for the open and closed structures, respectively. These values remain comparable with those characterizing a single emitter (see Table II). From the direct calculation of the electric field 0.25 nm above the three internal nanotubes (i.e., those of the middle of Fig. 2), we find 2.13 for the open tubes and 2.10 for the closed ones. When considering the three other tubes (i.e., those at the corners in the right part of Fig. 2), we find 2.28 for the open tubes and 3.54 for the closed ones. The reduction of the field-enhancement factor due to electrostatic interactions between the tubes is therefore stronger than that suggested from the Fowler-Nordheim analysis, especially for the internal tubes. If more nanotubes were considered, we expect the internal part of the bundle and the corresponding field-enhancement factors to be more affected by those interactions.[13]

IV. DISCUSSION

We calculated the total current emitted by bundles of open and closed (5,5) nanotubes, using a scattering technique that takes into account the details of the tubes' atomic configuration and surface barrier. This latter was computed by considering the atomic polarizabilities and the electrostatic interactions between neighboring structures. The simulations were achieved for either one, three, or six nanotubes, either open or closed, and for three values of the extraction field. Despite the complexity of the field-emission process and the diversity of the systems considered, it turns out that all our data can be cast into the following simple formula:

$$I_{\text{tot}} = I_{\text{isolated}} nb \times \exp[-a\sqrt{nb-1}], \tag{2}$$

where I_{tot} is the total current emitted by a bundle of nb nanotubes and I_{isolated} is the current emitted by an isolated tube. This is demonstrated in Fig. 10, where we represented $\ln[I_{\text{tot}}/(I_{\text{isolated}}nb)]$ as a function of $\sqrt{nb-1}$ for each type of nanotube and each value of the extraction field. Indeed, one can see that this representation of our data gives a perfect alignment for each series. The best linear fit of the average values is associated with the parameter $a=2.5179$. One can check that Eq. (2) used with this value of a reproduces the conclusions obtained in the previous section for the variations in current as the number of emitters increases.

Equation (2) can be interpreted in the following way: the first two factors describe the fact that the total emission is proportional to the number of emitters while the exponential factor stands for the screening due to the $n-1$ neighbors of each tube. The square root of $n-1$ has to be taken, since the efficiency of the screening depends on the number of tubes in each direction (n being the number of tubes on a surface). Since the field-enhancement factor is larger at the border of the bundles, the electronic emission from the outer tubes is more important than that from the inner ones. We may, however, consider $I_{\text{isolated}}nb$ as an average value and $\exp[-a\sqrt{nb-1}]$ as a first-order correction. In the case of nb isolated nanotubes, Eq. (2) is exact provided $a=0$ (no screening). For bundles with more than six nanotubes, additional corrections may be necessary and in particular one may have to consider the inner and outer tubes separately (we expect actually the emission from the inner part to be-

come negligible compared to that of the outer one). In its present form, however, Eq. (2) fits our data perfectly.

The results in Fig. 10 indicate that the slope a decreases proportionally to the applied electric field F, the data points associated with high fields being above those associated with lower ones. This tendency can be explained by the fact that at high fields the surface barrier is thinner and therefore less affected by the neighboring tubes than at low fields. The best fit we could find for the dependence is $a=a_0+a_1F$, where F is in V/nm and the two parameters a_0 and a_1 are 3.8 and -0.43 for the open tubes and 3.2 and -0.90 for the closed ones (note that the range of validity of this law is limited, since a must remain positive). The values of a_1 thus confirm that the dispersion around the average currents is higher for closed tubes than for open ones.

Assuming that the Fowler-Nordheim theory accurately describes the emission of a single tube, I_{isolated} then depends on $F^2\exp[-b/F]$. The presence of additional tubes introduces a new factor in the expression of the total current, which has the form $\exp[-a_1\sqrt{nb-1}F]$. Since this new dependence on F cannot be incorporated in the original equation, these results suggest that the Fowler-Nordheim theory would apply badly to bundles of nanotubes in conditions where $F^2 > b/(a_1\sqrt{nb-1})$. For bundles of six closed carbon nanotubes, the critical field is around 3.5 V/nm. Other reservations on the applicability of the Fowler-Nordheim equation to carbon nanotubes can be found in Refs. 33 and 34.

Besides total currents, the technique also provides the detailed energy distribution of the emitted electrons. Their main contribution is around the Fermi level and decreases as additional emitters are considered. The distributions also tend to be thinner and peaks associated with stationary waves in the body of the emitter less pronounced. These effects are due to the surface barrier, which becomes higher as the number of emitters increases. The most interesting result comes from the peaks associated with quasilocalized states. Their position indeed reflects the bundles' configuration, as we observed shifts of 0.45 and 0.65 eV relative to their initial position when increasing the number of tubes from one to three or six. These displacements seem proportional to the square root of nb and suggest that they may be used as indicator of the tubes' environment (reflecting the number of tubes or their spacing), provided an appropriate calibration is achieved.

V. CONCLUSION

We presented simulations of field emission from bundles of open and closed (5,5) nanotubes, using a transfer-matrix methodology for consideration of three-dimensional aspects of the structures and potential energy. In all cases, the closed nanotubes are found to emit less current than the open ones and to be more sensitive to the extraction field in their response to neighboring structures. Our results indicate that the bundles' total emission can be related to that of the isolated tubes by a simple empirical relation. The formula, which incorporates the number of tubes and the extraction field, suggests a deviation from the Fowler-Nordheim theory at high fields. In addition to the total current, the method provides the energy distribution of the emitted electrons. In situations where quasilocalized states are manifested by peaks in these distributions, it turns out that their position can be used as an indicator of the tubes' environment.

ACKNOWLEDGMENTS

This work was supported by the National Fund for Scientific Research (FNRS) of Belgium and by NSF Grant No. DMI-0078637 administrated by UHV Technologies, Inc., Mt. Laurel, NJ. One of the authors (A.M.) acknowledges the use of the Namur Scientific Computing Facility and the Belgian State Interuniversity Research Program on ''Quantum size effects in nanostructured materials'' (PAI/IUP P5/01). The authors are grateful to M. Devel for useful discussions.

*Corresponding author, electronic address: alexandre.mayer@fundp.ac.be

[1] W.A. de Heer, A. Châtelain, and D. Ugarte, Science **270**, 1179 (1995).
[2] J.M. Bonard, J.P. Salvetat, T. Stöckli, L. Forró, and A. Châtelain, Appl. Phys. A: Mater. Sci. Process. **69**, 245 (1999), and references therein.
[3] M.J. Fransen, Th.L. van Rooy, and P. Kruit, Appl. Surf. Sci. **146**, 312 (1999), and references therein.
[4] P.G. Collins and A. Zettl, Phys. Rev. B **55**, 9391 (1997).
[5] Ch. Adessi and M. Devel, Phys. Rev. B **62**, 13 314 (2000).
[6] K.A. Dean, O. Gröning, O.M. Küttel, and L. Schlapbach, Appl. Phys. Lett. **75**, 2773 (1999).
[7] R. Tamura and M. Tsukada, Phys. Rev. B **52**, 6015 (1995).
[8] D.L. Carroll, P. Redlich, P.M. Ajayan, J.C. Charlier, X. Blase, A. De Vita, and R. Car, Phys. Rev. Lett. **78**, 2811 (1997).
[9] A. De Vita, J.Ch. Charlier, X. Blase, and R. Car, Appl. Phys. A: Mater. Sci. Process. **68**, 283 (1999).
[10] Ph. Kim, T.W. Odom, J.L. Huang, and C.M. Lieber, Phys. Rev. Lett. **82**, 1225 (1999).
[11] S. Han and J. Ihm, Phys. Rev. B **61**, 9986 (2000).
[12] M.S.C. Mazzoni, H. Chacham, P. Ordejon, D. Sanchez-Portal, J.M. Soler, and E. Artacho, Phys. Rev. B **60**, 2208 (1999).
[13] L. Nilsson, O. Gröning, C. Emmenegger, O. Küttel, E. Schaller, L. Schlapbach, H. Kind, J.-M. Bonnard, and K. Kern, Appl. Phys. Lett. **76**, 2071 (2000).
[14] Ch. Adessi and M. Devel, Phys. Rev. B **65**, 075418 (2002).
[15] A. Mayer, N.M. Miskovsky, and P.H. Cutler, J. Vac. Sci. Technol. B **20**, 100 (2002).
[16] A. Mayer, N.M. Miskovsky, and P.H. Cutler, Appl. Phys. Lett. **79**, 3338 (2001).
[17] A. Mayer, N.M. Miskovsky, and P.H. Cutler, Ultramicroscopy **92**, 215 (2002).
[18] A. Mayer, N.M. Miskovsky, and P.H. Cutler, Phys. Rev. B **65**, 155420 (2002).
[19] A. Mayer, N.M. Miskovsky, and P.H. Cutler, Phys. Rev. B **65**, 195416 (2002).
[20] A. Mayer, N.M. Miskovsky, and P.H. Cutler, J. Phys.: Condens. Matter **15**, R177 (2003).
[21] A. Mayer, N.M. Miskovsky, and P.H. Cutler, J. Vac. Sci. Technol.

B **21**, 1545 (2003).
[22] D. Lovall, M. Buss, E. Graugnard, R.P. Andres, and R. Reifenberger, Phys. Rev. B **61**, 5683 (2000).
[23] A. Mayer and J.-P. Vigneron, Phys. Rev. B **56**, 12 599 (1997).
[24] A. Mayer and J.-P. Vigneron, J. Phys.: Condens. Matter **10**, 869 (1998); Phys. Rev. B **60**, 2875 (1999); Phys. Rev. E **59**, 4659 (1999); **61**, 5953 (2000).
[25] A. Mayer, P. Senet, and J-P. Vigneron, J. Phys.: Condens. Matter **11**, 8617 (1999).
[26] G.B. Bachelet, H.S. Greenside, G.A. Baraff, and M. Schlüter, Phys. Rev. B **24**, 4745 (1981).
[27] M. Devel, C. Girard, and C. Joachim, Phys. Rev. B **53**, 13 159 (1996).
[28] W. Liang, M. Bockrath, D. Bozovic, J.H. Hafner, M. Tinkham, and H. Park, Nature (London) **441**, 665 (2001).
[29] J. Luo, L.-M. Peng, Z.Q. Xue, and J.L. Wu, Phys. Rev. B **66**, 155407 (2002).
[30] R.H. Fowler and L. Nordheim, Proc. R. Soc. London, Ser. A **119**, 173 (1928).
[31] R.H. Good and E. Müller, *Field Emission*, in Handbook of Physics, Vol. 21 (Springer-Verlag, Berlin, 1956), pp. 176–231.
[32] P.H. Cutler, J. He, N.M. Miskovsky, T.E. Sullivan, and B. Weiss, J. Vac. Sci. Technol. B **11**, 387 (1993).
[33] J.-M. Bonard, M. Croci, I. Arfaoui, O. Noury, D. Sarangi, and A. Châtelain, Diamond Relat. Mater. **11**, 763 (2002).
[34] S. Han and J. Ihm, Phys. Rev. B **66**, 241402(R) (2002).